DOI: 10.1002/ejic.200600009

Transformation of a Tetranuclear Copper(II) Complex Bridged by Sugar Phosphates into Nucleotide-Containing Cu_4 Aggregations

Merii Kato,[a] Ajay Kumar Sah,[a] Tomoaki Tanase,*[a] and Masahiro Mikuriya[b]

Keywords: Coordination chemistry / Copper / Nucleic acids / Carbohydrates / Clusters

Reaction of $[Cu_4(\mu\text{-OH})\{\mu\text{-}(\alpha\text{-D-Glc-1P})\}_2(L)_4(H_2O)_2]X_3$ (**1a**: L = bpy, X = NO_3, α-D-Glc-1P = α-D-glucopyranose-1-phosphate) with $Na_2[H_2ATP]$ (ATP = adenosine 5′-triphosphate) readily afforded the ATP-bridged tetranuclear copper(II) complex $[Cu_4(\mu\text{-ATP})_2(bpy)_4]$ (**3**), which was characterized by X-ray crystallographic analysis to consist of four linearly dispersed $\{Cu^{II}(bpy)\}^{2+}$ fragments bridged by two triphosphate groups of the ATP tetravalent anions. The sugar and adenine base parts of the ATP moieties are away from the copper(II) centers, but the structure was stabilized by weak intramolecular π–π stacking between the ATP purine ring and two bpy ligands and intermolecular hydrogen bonding between the adenine base pairs. The variable-temperature magnetic susceptibility of complex **3** exhibited only weak antiferromagnetic couplings between the four linearly dispersed Cu^{II} ions. A similar reaction of **1a** or **2** (L = phen, X = NO_3) with Na_2[IMP] (IMP = inosine 5′-monophosphate) yielded a different type of tetracopper(II) complex formulated as $[Cu_4\{\mu\text{-(IMP-H)}\}_2(L)_4(H_2O)_4](NO_3)_2$ [L = bpy (**5**), phen (**6**)], in which the IMP moieties are deprotonated at the N-1 position of the nucleobase, forming IMP-H trianions, and four $\{Cu(bpy)(H_2O)\}^{2+}$ fragments are connected through the N-1, N-7, and O-6 atoms of the nucleobase and the monodentate 5′-phosphate group. Reaction of **1b** (L = bpy, X = Cl) with Na_2[UMP] (UMP = uridine 5′-monophosphate) resulted in a polymeric compound formulated as $\{[Cu\{\mu\text{-(UMP-H)}\}(bpy)(H_2O)]_2[Cu_4(\mu\text{-OH})\{\mu\text{-}(\alpha\text{-D-Glc-1P})\}_2(bpy)_4(H_2O)_2]Cl\}_n$ (**7**). The N-3 deprotonated $[UMP\text{-}H]^{3-}$ anions connect $\{Cu(bpy)(H_2O)\}^{2+}$ fragments through the N-3 nitrogen atom and the phosphate oxygen atoms to afford C_2-helical coordination polymers and the tetracopper(II) complex cations, $[Cu_4(\mu\text{-OH})\{\mu\text{-}(\alpha\text{-D-Glc-1P})\}_2(bpy)_4(H_2O)_2]^{3+}$, are incorporated between the polymer chains with a C_2-chiral arrangement of the $\{Cu_4(\mu\text{-OH})(\mu\text{-}PO_4)_2(bpy)_4(H_2O)_2\}$ framework constrained to the *Λ*-form through inter- and intramolecular stacking interactions between the bpy ligands.

Introduction

The interaction of metal ions with nucleotides and polynucleotides (DNA and RNA) has been extensively studied with a variety of bioinorganic interests, concerning metalloenzymes that promote cleavage of nucleotide phosphate ester bonds, such as DNA polymerase I (Mg^{2+}, Mn^{2+}, Zn^{2+}), P1 nuclease (Zn^{2+}), and RNase H (Mg^{2+}, Mn^{2+}), and so forth,[1] a number of bioenergetic processes coupled with phosphoryl transfer reactions of high-energy nucleotides, usually adenosine triphosphate (ATP), mediated by metal ions (Mg^{2+}, Mn^{2+}, etc.),[2] and the action of Pt^{II} complexes as anticancer drugs,[3] and so on. To elucidate the nucleotide–metal interaction in such biological processes, a number of binary and ternary transition-metal complexes involving nucleotides have been reported; however, most are mononuclear complexes or polymeric compounds containing mononuclear metal centers.[4] Whereas nucleotides are potentially ambivalent with their multiple metal-binding sites, phosphate groups, hydroxy groups of the sugar moiety, and nitrogen and oxygen atoms of the nucleobase, studies of discrete, multinuclear transition-metal complexes with nucleotides have been extremely scarce thus far. As to the complexes of nucleotides having di- and triphosphate groups, successfully isolated multimetallic complexes are only two examples with dinuclear Zn^{2+} and Cu^{2+} systems, $[Zn_2(\mu\text{-}H_2ATP)_2(bpy)_2]$ (**8**)[5] and $[Cu_2(\mu\text{-}H_2ATP)_2(phen)_2]$ (**9**)[6] (bpy = 2,2′-bipyridyl, phen = 1,10-phenanthroline). The reason for the lack of studies may not only be the difficulty of getting crystalline compounds because of their ambivalent properties, but also the fact that most divalent metal ions catalyze the nonenzymatic hydrolysis of the nucleotide phosphate groups. Notably, one of the best characterized DNA cleavage reactions is that promoted by $[Cu(phen)_2]^{2+}$.[7] Even for thermodynamically stable nucleoside monophosphate esters, a very restricted number of structures are available for multinuclear transition-metal complexes, $[Cu_4\{\mu\text{-(IMP-H)}\}(phen)_4(H_2O)_2](NO_3)_2$ (**6**, IMP-H = N-1 deprotonated inosine 5′-monophosphate),[8] $[\{Ru(\mu\text{-AMP})(\eta^6\text{-}p\text{-}MeC_6H_4iPr)\}_3]$ (AMP = adenosine 5′-monophosphate),[9] $Na_2[Mo_5O_{15}(\mu\text{-HAMP})_2]$,[10] and

[a] Department of Chemistry, Faculty of Science, Nara Women's University,
Kitauoya-higashi-machi, Nara 630-8285, Japan
Fax: +81-742-20-3399
E-mail: tanase@cc.nara-wu.ac.jp
[b] Department of Chemistry, School of Science and Technology, Kwansei Gakuin University,
2-1 Gakuen, Sanda-shi, Hyogo 669-1337, Japan

$[Mo_2(\eta^5\text{-}C_5H_5)_4(\mu\text{-dGMP})_2]$ (dGMP = 2′-deoxyguanosine 5′-monophosphate),[11] and for dicopper(II) complexes involving the $\{LCu(\mu\text{-}OPO)_2CuL\}$ eight-membered macrocycles with nucleoside 5′-monophosphates [L = bpy, phen, and bis(2-pyridyl)amine].[12]

Recently, we synthesized a tetranuclear copper(II) complex bridged by α-D-glucose-1-phosphate (α-D-Glc-1P) dianions, $[Cu_4(\mu\text{-OH})\{\mu\text{-}(\alpha\text{-D-Glc-1P})\}_2(L)_4(H_2O)_2]X_3$ [L = bpy, X = NO_3 (**1a**), Cl (**1b**), Br (**1c**); L = phen, X = NO_3 (**2**)] (Figure 1a).[13] Complex **2** was structurally characterized as the first example of a transition-metal complex containing free sugar monophosphates, in which four $\{Cu(phen)\}^{2+}$ fragments are held together by a hydroxo bridge and two phosphate groups of α-D-Glc-1P moieties to result in a trapezoidal Cu^{II}_4 framework with the D-glucopyranosyl pendants away from the metal centers.[13] In the crystal structure of **2**, two C_2-chiral structures with respect to the arrangement of bpy ligands, *Δ* (cation A) and *Λ* (cation B), were observed in a 1:1 ratio; both are coupled to a different orientation of α-D-glucopyranosyl pendants, upward and downward, respectively (Figure 1b, c). In addition, complex **1a** was found to readily undergo a phosphate ester exchange reaction and be transformed into an ATP-stabilized tetracopper(II) complex, $[Cu_4(\mu\text{-ATP})_2(bpy)_4]$ (**3**). These results prompted us to investigate the reactions of **1** and **2** with several nucleotides. In the present study, we wish to report the full details of synthesis and characterization of **3**, together with those for $[Cu_4\{\mu\text{-}(IMP\text{-}H)\}_2(L)_4(H_2O)_4](NO_3)_2$ [L = bpy (**5**), phen (**6**)] and the polymeric compound formulated as $\{[Cu\{\mu\text{-}(UMP\text{-}H)\}(bpy)(H_2O)]_2[Cu_4(\mu\text{-OH})\{\mu\text{-}(\alpha\text{-D-Glc-1P})\}_2(bpy)_4(H_2O)_2]Cl\}_n$ (**7**, UMP-H = N-3 deprotonated uridine 5′-monophosphate). Although the structure of **3** was briefly reported,[13a] the detailed ATP-bridging structure in **3** compared with related compounds and its magnetic property are presented in this report. The present reaction may also provide an efficient route to a series of tetranucler ternary Cu^{II} complexes with IMP moieties and diimine auxiliary ligands. In addition, the structure of **7** revealed an interesting chiral influence transfer from the C_2-helical structure of the polymer $\{[Cu\{\mu\text{-}(UMP\text{-}H)\}(bpy)(H_2O)]^-\}_n$ to the C_2-chiral structure of the tetranuclear Cu^{II} units involved in **7**, $[Cu_4(\mu\text{-OH})\{\mu\text{-}(\alpha\text{-D-Glc-1P})\}_2(bpy)_4(H_2O)_2]^{3+}$, through inter- and intramolecular bpy–bpy stacking interactions.

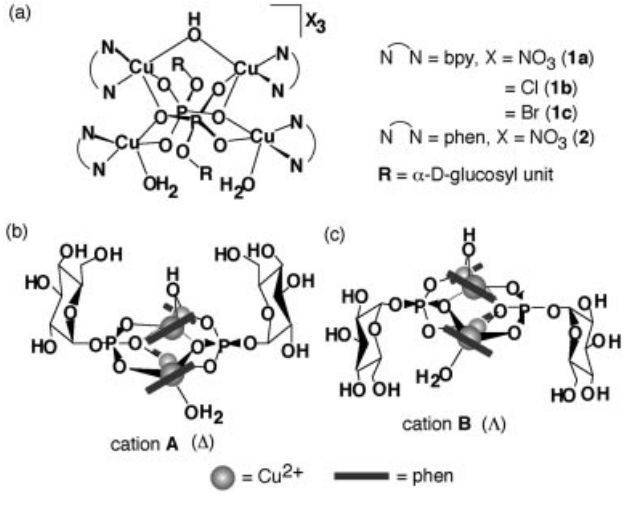

Figure 1. (a) Structure of **1a**–**c** and **2**. Schematic structures for (b) cation **A** and (c) cation **B** involved in **2**. Gray bars represent the phen ligands which are arranged in *Δ* and *Λ* configurations with respect to the pseudo-C_2 axis for cations **A** and **B**, respectively.

Results and Discussion

Synthesis and Structure of $[Cu_4(\mu\text{-ATP})_2(bpy)_4]$ (3)

When the tetranuclear copper(II) complex bridged by a sugar phosphate, $[Cu_4(\mu\text{-OH})\{\mu\text{-}(\alpha\text{-D-Glc-1P})\}_2(bpy)_4(H_2O)_2](NO_3)_3$ (**1a**), was treated with $Na_2[H_2ATP]$ in a 1:2 ratio at room temperature, a phosphate ester exchange reaction readily proceeded to result in the formation of an ATP-bridged tetracopper(II) complex, $[Cu_4(\mu\text{-ATP})_2(bpy)_4]$ (**3**), in good yield (56%) and crystalline form (Scheme 1).

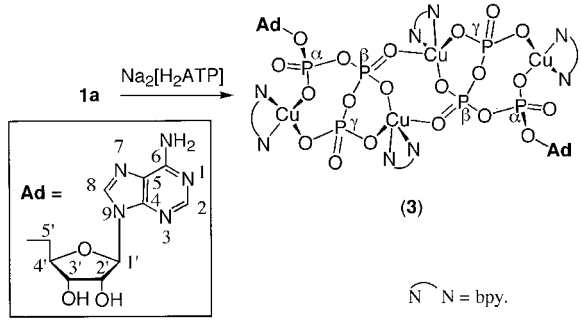

Scheme 1.

The IR spectrum showed the presence of ATP anions and bpy ligands, and the CD spectral pattern around the d–d transition region for Cu^{II} ions is quite different from that of the starting complex **1a**, indicating an introduction of ATP on the tetranuclear centers. From the mother liquor, a very small amount of a pyrophosphate-bridged dicopper complex, $[Cu_2(\mu\text{-}P_2O_7)(bpy)_2(H_2O)_2]$ (**4**),[14] was obtained, suggesting that hydrolytic cleavage of the triphosphate group occurred to a small extent during the reaction. It should be noted that complex **3** was not obtained just by mixing $Cu(NO_3)_2{\cdot}3H_2O$ with $Na_2[H_2ATP]$ and bpy, demonstrating that the tetranuclear Cu^{II} centers of **1a** provide a suitable platform to stabilize the triphosphate unit of ATP.

The structure of **3** was determined by X-ray crystallographic analysis; an ORTEP plot with the atomic numbering scheme is given in Figure 2a and selected bond lengths and angles are listed in Table 1. The structure consists of four linearly dispersed $\{Cu^{II}(bpy)\}^{2+}$ fragments bridged by two ATP tetravalent anions with interatomic distances of Cu1···Cu2 = 3.444(1) Å, Cu3···Cu4 = 3.4523(8) Å, and Cu2···Cu4 = 5.0613(7) Å. The triphosphate group of ATP exclusively connects two Cu^{II} ions, each ligated by a bpy ligand, to afford the square-planar dicopper(II) unit, $\{Cu_2(\mu\text{-ATP})(bpy)_2\}$. The adenine bases and D-ribofuranosyl parts are away from the metal centers without any inter-

actions. The two dinuclear fragments are further connected through the axial coordination of β-phosphate oxygen atoms [Cu2–O23 = 2.263(4) Å, Cu4–O10 = 2.247(4) Å], resulting in a characteristic eight-membered puckered ring of the central part (Figure 2b). Whereas metal complexes with ATP could provide useful insights to elucidate bioenergetic processes, characterized examples are still rare and most are mononuclear species[15] and their sodium salts.[16] In particular, those containing multimetallic centers are strictly limited; the only available structures with multinuclear transition-metal ions are the dinuclear complexes $[Zn_2(\mu\text{-}H_2ATP)_2(bpy)_2]$ (**8**)[5] and $[Cu_2(\mu\text{-}H_2ATP)_2(phen)_2]$ (**9**),[6] and with the present complex **3** the first crystal structure of a tetranuclear transition-metal complex with ATP anions is available. Both complexes **8** and **9** possess an essentially identical structure with the triphosphate group chelating to a metal ion through the three α-, β-, and γ-phosphate oxygen atoms in a facial mode, and another γ-phosphate oxygen atom attached to the other metal ion, forming an $[MOPO]_2$ eight-membered macrocycle. The metal centers adopt an $[N_2O_4]$ octahedral geometry. In contrast, in the present structure, the bridging behavior of the ATP triphos-

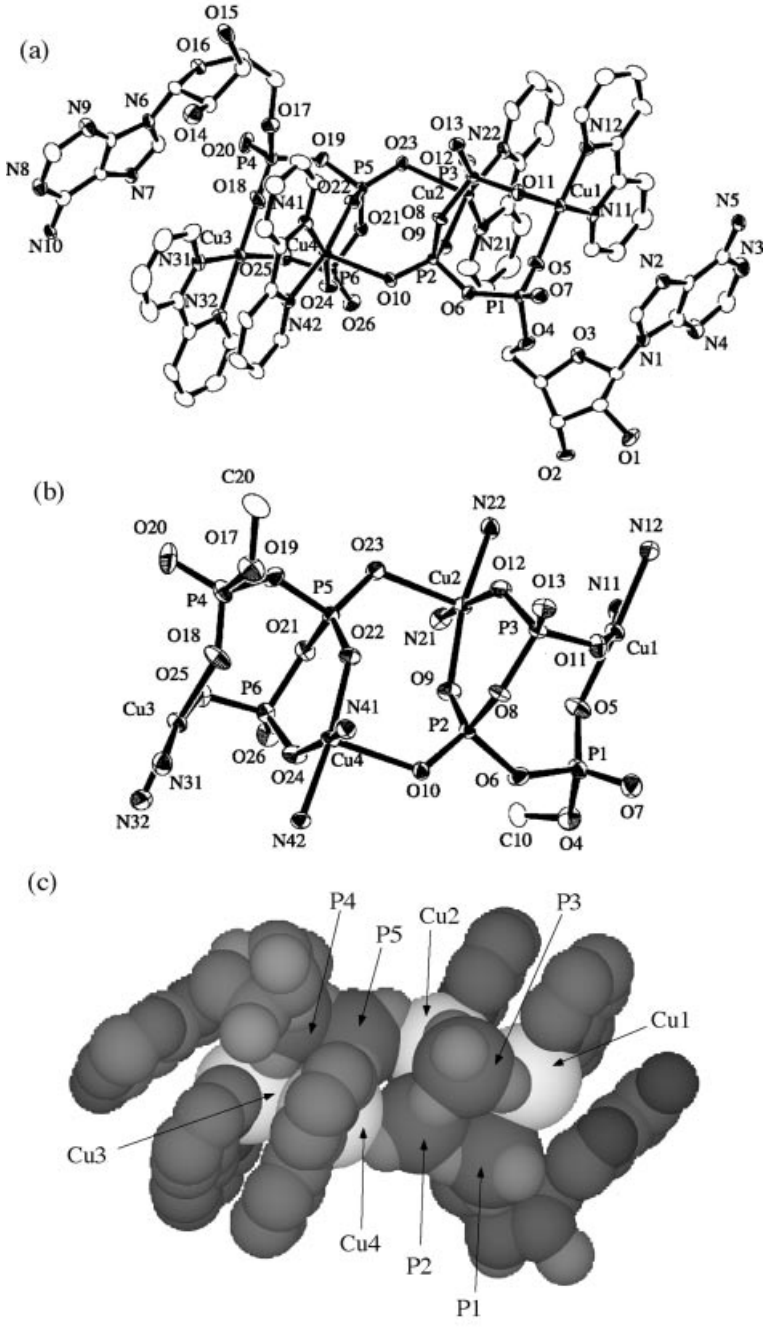

Figure 2. (a) ORTEP plot of **3** with hydrogen atoms omitted for clarity. (b) Core structure of **3**; the adenosine parts and the carbon atoms of bpy ligands are omitted. (c) Perspective drawing of **3** with van der Waals radii.

Table 1. Selected bond lengths [Å] and angles [°] for complex **3**.

Cu1–O5	1.943(4)	Cu3–O18	1.922(4)
Cu1–O11	1.951(4)	Cu3–O25	1.919(4)
Cu1–N11	1.983(5)	Cu3–N31	2.021(4)
Cu1–N12	1.978(4)	Cu3–N32	2.006(5)
Cu2–O9	1.982(4)	Cu4–O10	2.247(4)
Cu2–O12	1.934(4)	Cu4–O22	1.935(4)
Cu2–O23	2.263(4)	Cu4–O24	1.921(4)
Cu2–N21	1.980(4)	Cu4–N41	2.011(4)
Cu2–N22	1.973(5)	Cu4–N42	2.032(4)
P1–O4	1.582(4)	P4–O17	1.580(4)
P1–O5	1.496(5)	P4–O18	1.501(5)
P1–O6	1.592(4)	P4–O19	1.600(4)
P1–O7	1.487(4)	P4–O20	1.471(5)
P2–O6	1.611(5)	P5–O19	1.602(5)
P2–O8	1.583(3)	P5–O21	1.577(4)
P2–O9	1.488(4)	P5–O22	1.503(4)
P2–O10	1.490(3)	P5–O23	1.487(3)
P3–O8	1.644(3)	P6–O21	1.637(4)
P3–O11	1.519(4)	P6–O24	1.520(5)
P3–O12	1.512(5)	P6–O25	1.534(4)
P3–O13	1.497(4)	P6–O26	1.482(4)
O5–Cu1–O11	91.0(2)	O18–Cu3–O25	92.8(2)
N11–Cu1–N12	82.0(2)	N31–Cu3–N32	80.5(2)
O9–Cu2–O12	93.7(2)	O10–Cu4–O22	92.5(2)
O9–Cu2–O23	97.5(1)	O10–Cu4–O24	91.6(2)
O12–Cu2–O23	88.4(2)	O22–Cu4–O24	95.2(2)
N21–Cu2–N22	81.5(2)	N41–Cu4–N42	80.2(2)
O5–P1–O6	109.4(2)	O18–P4–O19	110.7(2)
O6–P2–O8	103.4(2)	O19–P5–O21	102.8(2)
O6–P2–O9	109.4(2)	O19–P5–O22	109.1(2)
O8–P2–O9	111.2(2)	O21–P5–O22	111.3(2)
O8–P3–O11	106.5(2)	O21–P6–O24	106.4(2)
O8–P3–O12	106.7(2)	O21–P6–O25	105.1(2)
O11–P3–O12	111.8(2)	O24–P6–O25	110.7(2)
Cu1–O5–P1	132.8(2)	Cu3–O18–P4	135.0(3)
P1–O6–P2	133.6(3)	P4–O19–P5	131.0(3)
P2–O8–P3	128.7(2)	P5–O21–P6	129.4(2)
Cu2–O9–P2	133.7(2)	Cu4–O22–P5	131.8(2)
Cu4–O10–P2	124.0(2)	Cu2–O23–P5	118.1(2)
Cu1–O11–P3	123.4(3)	Cu4–O24–P6	131.5(2)
Cu2–O12–P3	128.8(3)	Cu3–O25–P6	116.2(3)

phate group in the dimeric unit of **3** is remarkably different, as two Cu^{II} ions are held together by the bridges from α- and β-phosphate oxygen atoms [Cu1–O5 = 1.943(4) Å, Cu3–O18 = 1.922(4) Å; Cu2–O9 = 1.982(4) Å, Cu4–O22 = 1.935(4) Å] and from two oxygen atoms of the γ-phosphate unit [Cu1–O11 = 1.951(4) Å, Cu2–O12 = 1.934(4) Å; Cu3–O25 = 1.919(4) Å, Cu4–O24 = 1.921(4) Å], resulting in an unprecedented bridging structure of the ATP triphosphate group (Figure 2b). While the triphosphate backbones are folded, as indicated by the angles P1–P2–P3 = 86.11(4)° and P4–P5–P6 = 88.23(5)°, like complexes **8** and **9**, strain involved in the triphosphate parts of **3** might be released to some extent, in comparison with those in the dimers of **8** and **9** and the mononuclear complexes.[5,6,15] In complex **3**, the eight-membered chelate ring by the α- and γ-phosphate oxygen atoms is fused with the six-membered chelate ring by the β- and γ-oxygen atoms, which should be contrasted with two fused six-membered chelate rings from α-/β- and β-/γ-phosphate oxygen atoms in **8** and **9**. The $\{Cu_4(\mu\text{-}P_3O_{10})_2(bpy)_4\}$ core structure, except the adenosine moieties, possesses a pseudocentrosymmetry; the outer two copper ions (Cu1, Cu3) take an $[N_2O_2]$ square-planar geometry and the inner two (Cu2, Cu4) are in an $[N_2O_3]$ square-pyramidal environment with usual bond lengths and angles. It should be noted that, by using the $HADP^{2-}$ anion, a related tetranuclear copper(II) complex, $[Cu_4(\mu\text{-HADP})_2(NO_3)_2(bpy)_2(H_2O)_2]^{2+}$, was prepared and involves a central eight-membered macrocycle very similar to that of **3** (ADP = adenosine 5′-diphosphate).[17]

The adenosine residues take *anti*–C2′*–endo* conformation without any direct interaction with metal ions, but weak intramolecular π–π stacking between the purine ring and two bpy ligands is observed, as in complexes **8** and **9**.[5,6] The adenine–bpy and bpy–bpy intramolecular stacking interactions in **3** (Figure 2c) enhance its stability and may prevent coordination of the adenosine moieties to the metal centers. In the lattice packing, the N-7 imino and the N-6 amino groups of the adenine base are hydrogen-bonded to the same functional pair of ATP anchoring on the neighboring molecule [N2···N10* = 2.870(6) Å, N5···N7* = 2.980(6) Å; the atoms with * are generated by a symmetry operation of $x - 1$, y, $z + 1$], these hydrogen-bonding networks further stabilizing the ATP moieties trapped onto the tetracopper(II) aggregation.

The temperature-dependent magnetic susceptibility data for complex **3** are shown as plots of χ_M and μ_{eff} versus T over a range of 4.5–300 K (Figure 3), indicating a very weak antiferromagnetic interaction with μ_{eff} per Cu_4 of 4.24 μ_B (300 K) and 3.22 μ_B (4.5 K). The magnetic susceptibility data were fitted by a theoretical expression derived from the van Vleck equation with the J_1 and J_2 spin-exchange coupling constants [Equation (1)] to afford the best-fitted values of $g = 2.33$, $J_1 = -1.2$ cm^{-1}, and $J_2 = -3.1$ cm^{-1}. The results clearly demonstrate that antiferromagnetic spin-exchange couplings are not effective in the triphosphate-bridged dimer and interdimers, which was consistent with the structural features involving no effective pathway for metal-to-metal magnetic interactions.

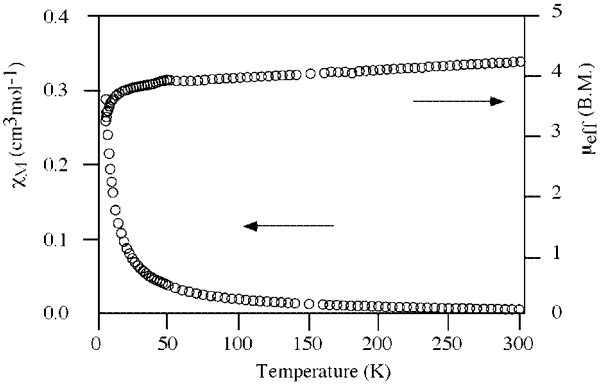

Figure 3. Plots of magnetic susceptibility (χ_M) and μ_{eff} vs. T for **3**.

Synthesis and Structure of $[Cu_4\{\mu\text{-(IMP-H)}\}_2(L)_4(H_2O)_4](NO_3)_2$ [L = bpy (5), phen (6)]

The tetranuclear copper complexes **1a** and **2** readily reacted with Na_2[IMP] in water to yield green block-shaped

crystals of $[Cu_4\{\mu\text{-}(IMP\text{-}H)\}_2(L)_4(H_2O)_4](NO_3)_2$ [L = bpy (**5**) 64%; phen (**6**) 26%], where the abbreviation of IMP-H represents the N-1 deprotonated inosine 5′-monophosphate trianion (Scheme 2). The IR spectral patterns of **5** and **6** are very similar, indicating the presence of IMP and nitrate anions as well as the diimine ligands. The circular dichroism spectra of **5** and **6** also resemble each other, suggesting incorporation of the nucleotide moieties into the tetranuclear Cu^{II} centers. The ESI mass spectra for aqueous solutions containing **5** and **6** exhibit divalent cationic peaks corresponding to $\{Cu_4(IMP\text{-}H)_2(L)_4\}^{2+}$ at 783.16 for **5** (L = bpy) and 831.14 for **6** (L = phen).

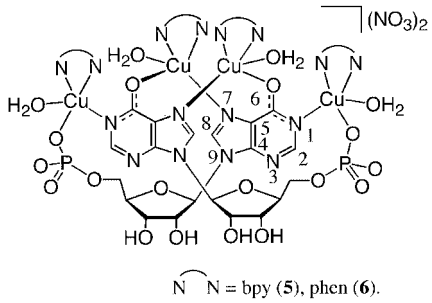

Scheme 2.

A detailed structure of **6** was determined by low-temperature X-ray crystallography using a CCD detector. As the present crystallographic structure for **6**·21.5H_2O is almost identical within the experimental errors to the structure for **6**·14H_2O reported by Bau,[8] except for the number of identified solvent water molecules, we wish to describe the structural features briefly as follows. An ORTEP plot for the complex cation of **6** with the atomic numbering scheme is given in Figure 4 and some selected bond lengths and angles are listed in Table 2. In the complex cation of **6**, four $\{Cu(phen)(H_2O)\}^{2+}$ fragments are held together by two inosine monophosphate anions to result in a pseudo-C_2-symmetrical structure [Cu1···Cu2 = 3.431(1) Å, Cu1···Cu3 = 4.232(1) Å, Cu2···Cu4 = 4.254(1) Å]. Each inosine monophosphate moiety is deprotonated at the N-1 position of the nucleobase and bridges four Cu^{II} ions

Table 2. Selected bond lengths [Å] and angles [°] for complex **6**.

Cu1–O5	1.943(4)	Cu3–O18	1.922(4)
Cu1–O1	2.175(4)	Cu2–O2	2.193(4)
Cu1–O21	1.980(4)	Cu2–O11	1.955(4)
Cu1–N2	2.018(4)	Cu2–N6	2.018(4)
Cu1–N11	2.010(5)	Cu2–N13	2.010(4)
Cu1–N12	2.015(4)	Cu2–N14	2.022(5)
Cu3–O3	2.225(4)	Cu4–O4	2.227(5)
Cu3–O16	1.943(4)	Cu4–O26	1.946(4)
Cu3–N7	2.021(5)	Cu4–N3	2.042(5)
Cu3–N15	2.024(5)	Cu4–N17	2.030(5)
Cu3–N16	2.023(5)	Cu4–N18	2.017(5)
P1–O15	1.623(4)	P2–O25	1.612(4)
P1–O16	1.534(4)	P2–O26	1.531(4)
P1–O17	1.520(4)	P2–O27	1.514(4)
P1–O18	1.508(4)	P2–O28	1.502(4)
O11–C13	1.263(7)	O21–C23	1.272(7)
N3–C13	1.365(7)	N7–C23	1.367(7)
N3–C14	1.350(8)	N7–C24	1.345(8)
O1–Cu1–O21	93.5(2)	O2–Cu2–O11	91.8(2)
O1–Cu1–N2	92.9(2)	O2–Cu2–N6	92.1(2)
O21–Cu1–N2	96.5(2)	O11–Cu2–N6	95.8(2)
N11–Cu1–N12	82.1(2)	N13–Cu2–N14	82.2(2)
O3–Cu3–O16	97.7(2)	O4–Cu4–O26	99.7(2)
O3–Cu3–N7	99.0(2)	O4–Cu4–N3	98.4(2)
O16–Cu3–N7	90.6(2)	O26–Cu4–N3	92.9(2)
N15–Cu3–N16	81.5(2)	N17–Cu4–N18	81.7(2)
O15–P1–O16	101.6(2)	O25–P2–O26	101.1(2)
Cu2–O11–C13	127.3(4)	Cu1–O21–C23	125.6(3)
Cu3–O16–P1	131.5(3)	Cu4–O26–P2	129.1(2)

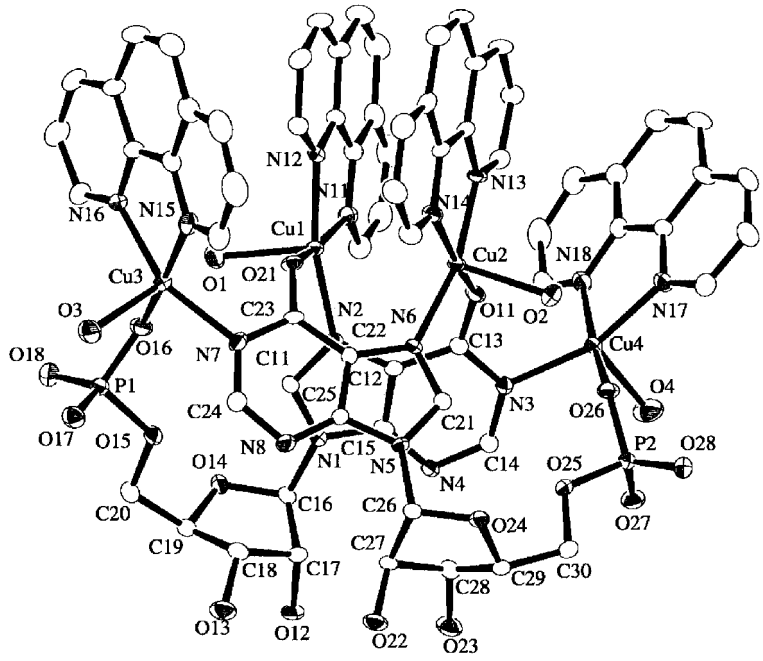

Figure 4. ORTEP plot of **6** with hydrogen atoms omitted for clarity.

through the deprotonated N-1 nitrogen atom [Cu3–N7 = 2.021(5) Å, Cu4–N3 = 2.042(5) Å], the oxygen atom at C-6 position [Cu1–O21 = 1.980(4) Å, Cu2–O11 = 1.955(4) Å], the N-7 nitrogen atom [Cu1–N2 = 2.018(4) Å, Cu2–N6 = 2.018(4) Å], and the monodentate phosphate oxygen atom [Cu3–O16 = 1.943(4) Å, Cu4–O26 = 1.946(4) Å]. There is no interaction between the D-ribose units and the metal centers. All four Cu^{II} ions take an $[N_3O_2]$ square-pyramidal coordination geometry with the water at its apical site (av. Cu–O = 2.205 Å). The structural features are essentially identical to those already reported.[8]

Transformation of 1b to $[Cu\{\mu\text{-}(UMP\text{-}H)\}(bpy)(H_2O)]_2[Cu_4(\mu\text{-}OH)\{\mu\text{-}(\alpha\text{-}D\text{-}Glc\text{-}1P)\}_2(bpy)_4(H_2O)_2]Cl$ (7)

When complex **1b** was treated with uridine 5′-monophosphate disodium salt (Na_2[UMP]) in water, blue crystals formulated as $[Cu\{\mu\text{-}(UMP\text{-}H)\}(bpy)(H_2O)]_2[Cu_4(\mu\text{-}OH)\{\mu\text{-}(\alpha\text{-}D\text{-}Glc\text{-}1P)\}_2(bpy)_4(H_2O)_2]Cl$ (**7**) were obtained in moderate yield (30%) (Scheme 3), which were characterized by elemental analysis, IR, UV/Vis, and CD spectroscopic data, and X-ray crystallographic analysis. The X-ray crystal structure revealed that compound **7** is composed of a dis-

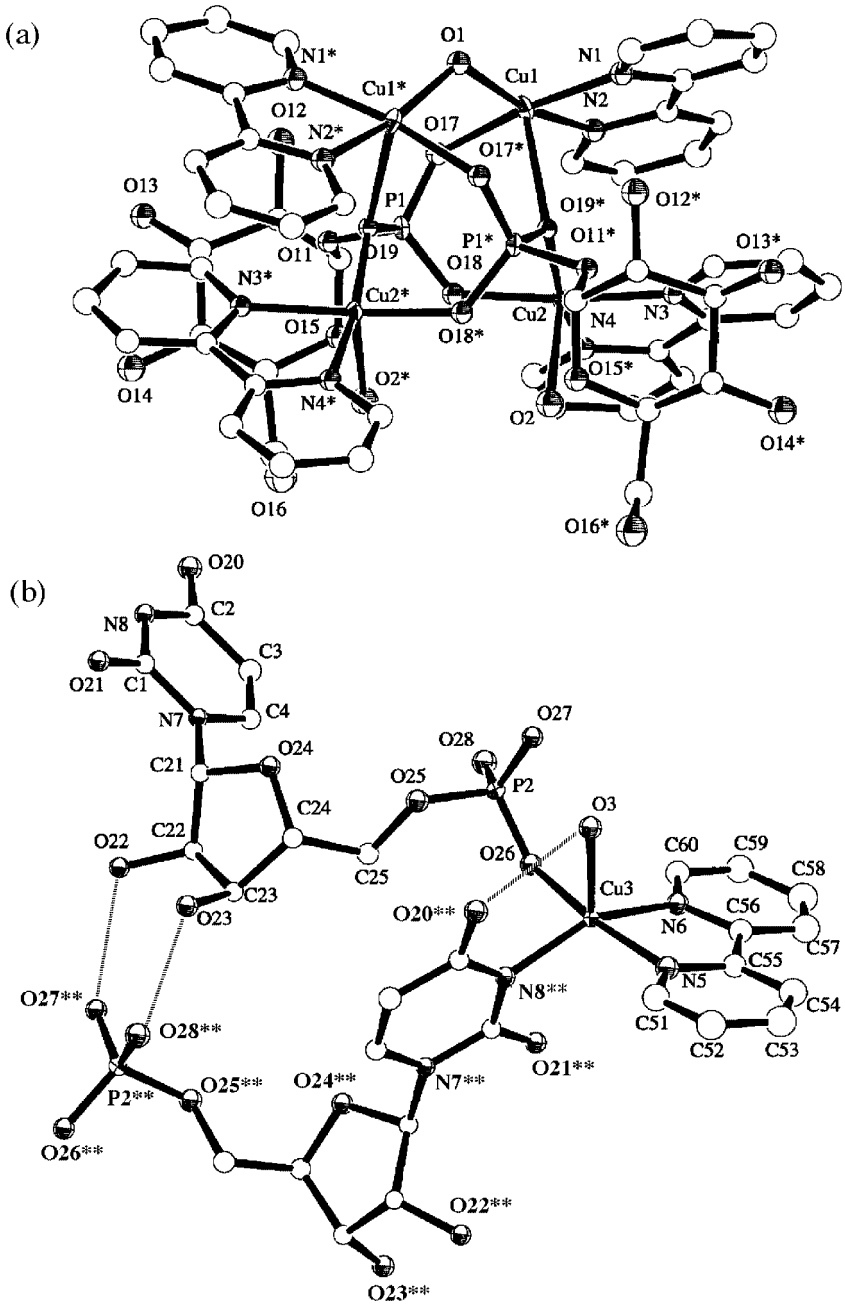

Figure 5. ORTEP diagrams for (a) the tetracopper(II) unit, $[Cu_4(\mu\text{-}OH)\{\mu\text{-}(\alpha\text{-}D\text{-}Glc\text{-}1P)\}_2(bpy)_4(H_2O)_2]^{3+}$, and (b) the polymer part, $\{[Cu\{\mu\text{-}(UMP\text{-}H)\}(bpy)(H_2O)]^-\}_n$, of **7**. Hydrogen atoms are omitted for clarity and hydrogen-bonding interactions are indicated by dotted thin lines.

Table 3. Selected bond lengths [Å] and angles [°] for complex **7**.[a]

Cu1–O1	1.911(5)	Cu3–O3	2.360(7)
Cu1–O17	1.967(7)	Cu3–O26	1.917(7)
Cu1–O19*	2.455(6)	Cu3–N5	2.015(9)
Cu1–N1	1.988(9)	Cu3–N6	1.997(9)
Cu1–N2	2.005(9)	Cu3–N8**	2.033(8)
Cu2–O2	2.270(9)	P2–O25	1.598(8)
Cu2–O18	1.961(7)	P2–O26	1.517(8)
Cu2–O19*	1.938(6)	P2–O27	1.520(7)
Cu2–N3	2.007(8)	P2–O28	1.523(7)
Cu2–N4	2.003(8)	O20–C2	1.27(1)
P1–O11	1.608(7)	O21–C1	1.25(1)
P1–O17	1.512(8)	N8–C1	1.33(1)
P1–O18	1.517(8)	N8–C2	1.38(1)
P1–O19	1.534(6)		
O1–Cu1–O17	90.7(3)	O3–Cu3–O26	93.9(3)
O1–Cu1–O19*	99.6(3)	O3–Cu3–N5	86.5(3)
O1–Cu1–N1	97.5(3)	O3–Cu3–N6	109.4(3)
O1–Cu1–N2	165.9(4)	O3–Cu3–N8**	97.1(3)
O17–Cu1–O19*	89.1(2)	O26–Cu3–N5	171.5(3)
O17–Cu1–N1	171.4(3)	O26–Cu3–N6	91.0(3)
O17–Cu1–N2	92.0(3)	O26–Cu3–N8**	92.3(3)
O19*–Cu1–N1	87.0(3)	N5–Cu3–N6	80.9(4)
O19*–Cu1–N2	94.3(3)	N5–Cu3–N8**	96.1(3)
N1–Cu1–N2	80.6(4)	N6–Cu3–N8**	153.0(3)
O2–Cu2–O18	95.7(3)		
O2–Cu2–O19*	95.2(3)		
O2–Cu2–N3	95.6(3)		
O2–Cu2–N4	99.0(3)		
O18–Cu2–O19*	91.9(3)		
O18–Cu2–N3	166.9(3)		
O18–Cu2–N4	90.5(3)		
O19*–Cu2–N3	93.8(3)		
O19*–Cu2–N4	165.3(3)		
N3–Cu2–N4	81.1(3)		
O11–P1–O17	108.6(4)	O25–P2–O26	107.2(4)
O11–P1–O18	105.1(4)	O25–P2–O27	102.5(4)
O11–P1–O19	103.8(4)	O25–P2–O28	108.1(4)
O17–P1–O18	112.5(4)	O26–P2–O27	114.6(4)
O17–P1–O19	112.4(4)	O26–P2–O28	109.5(4)
O18–P1–O19	113.6(4)	O27–P2–O28	114.2(4)
Cu1–O1–Cu1*	122.0(6)		
Cu1–O19*–Cu2	104.2(2)		

[a] Symmetry equivalents: *: $-x + 1, y, -z$; **: $-x + 1/2, y + 1/2, -z - 1$.

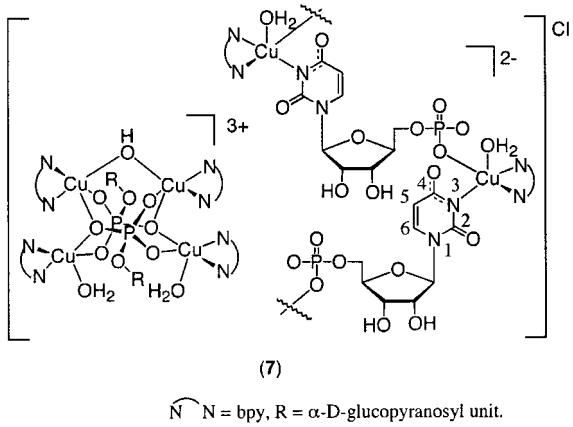

Scheme 3.

crete tetranuclear $[Cu_4(\mu\text{-}OH)\{\mu\text{-}(\alpha\text{-D-Glc-1P})\}_2(bpy)_4(H_2O)_2]^{3+}$ cation (Figure 5a), a coordination polymer with a $[Cu\{\mu\text{-}(UMP\text{-}H)\}(bpy)(H_2O)]^-$ monoanionic unit (Figure 5b), and a chloride anion, in a 1:2:1 ratio. Selected bond lengths and angles are listed in Table 3.

In the polymeric structure of $\{[Cu\{\mu\text{-}(UMP\text{-}H)\}(bpy)(H_2O)]^-\}_n$ (Figure 5b), the uridine 5′-monophosphate moieties are deprotonated at the N-3 position of the nucleobase to form the $[UMP\text{-}H]^{3-}$ trianions, which connect mononuclear Cu^{II} ions through the N-3 deprotonated nitrogen atom [Cu3–N8** = 2.033(8) Å] and the phosphate oxygen atom in a monodentate fashion [Cu3–O26 = 1.917(7) Å]. The Cu3···Cu3** interatomic distance is 12.170(2) Å. The Cu^{II} center is further ligated by two nitrogen atoms of bpy [Cu3–N5 = 2.015(9) Å, Cu3–N6 = 1.997(9) Å] and a water oxygen atom [Cu3–O3 = 2.360(7) Å] to complete a square-pyramidal $[N_3O_2]$ coordination geometry. The Cu atom deviates toward the apical O3 atom by 0.224(4) Å from the basal mean plane, and consequently the geometrical structure is deformed, with a τ value of 0.31.[18] On the basis of the N–C and O–C bond lengths, the negative charge generated upon N-3 deprotonation should be delocalized in the neighboring O-4 and O-2 oxygen atoms, and notably, the O-4 oxygen atom is hydrogen-bonded to the apical water ligand [O3···O20** = 2.76(1) Å], and the O-2 oxygen atom weakly interacts with the Cu ion at the sixth semi-coordination site [Cu3···O21** = 2.732(7) Å]. These structural features may contribute to fix the uracil base orientation with respect to the copper center. The polymeric structure is further supported by the intrapolymer hydrogen-bonding interaction between the two hydroxy groups of the D-ribofuranosyl unit and the two oxygen atoms of the phosphate group [O22···O27** = 2.68(1) Å, O23···O28** = 2.57(1) Å]. The overall structure of the polymer possesses a C_2-helical symmetry along the *b* axis, as illustrated in Figure 6.

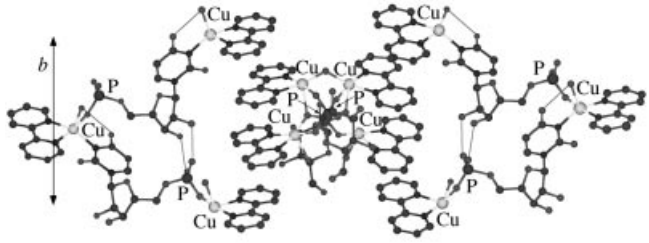

Figure 6. Perspective drawing for a part of the packing structure of **7** viewed vertically to the *b*-axis, showing the stacking interactions between the bpy ligands bound to the polymeric and the tetranuclear Cu^{II} units.

The tetracopper(II) complex cation (Figure 5a), $[Cu_4(\mu\text{-}OH)\{\mu\text{-}(\alpha\text{-D-Glc-1P})\}_2(bpy)_4(H_2O)_2]^{3+}$, has a crystallographically imposed C_2 symmetry with the axis passing through the O1 atom and the middle point between the Cu1 and Cu1* atoms, and is comprised of four Cu^{II} ions bridged by a hydroxo and two α-D-glucose-1-phosphate dianions together with auxiliary ligations of four bpy and two water molecules. The tetracopper framework is trapezoidal in which the upper two Cu atoms are connected by μ-OH and

two μ-1,3-OPO′ bridges, the basal two Cu atoms by two μ-1,3-OPO′ bridges, and the upper and basal Cu pairs by μ-1,1-O and μ-1,3-OPO′ bridges of the phosphate groups [Cu1···Cu1* = 3.342(3) Å, Cu1···Cu2 = 3.480(2) Å, Cu2···Cu2* = 4.366(2) Å]. An intramolecular π–π stacking interaction between the bpy ligands bound to the upper and basal metal ions is observed, as in complex **2** with phen ligands. The structure is essentially similar to those observed in the crystal structure of **2**,[13] except the C_2-chiral structures of the $\{Cu_4(\mu\text{-}OH)(\mu\text{-}PO_4)_2(L)_4(H_2O)_2\}$ core depending on the orientation of sugar pendants. Without any chiral molecules other than the sugar phosphate as in **2**, two enantiomeric structures arose (Figure 1b, c) presumably to avoid steric repulsive interaction between the sugar pendants and phen moieties and to increase the π–π stacking stabilization of phen ligands. In the present case of **7**, the observed C_2 configuration is *Λ* with downward orientation of the sugar pendants; the C-6 hydroxymethyl groups of the sugar residues are away from the upper $Cu_2(\mu\text{-}OH)$ unit. Namely, only one C_2-chiral structure of the tetracopper complex cation is stabilized through interaction with the coordination polymers containing the chiral biomolecule UMP linkers. As shown in Figure 6, the $\{[Cu\{\mu\text{-}(UMP\text{-}H)\}(bpy)(H_2O)]^-\}_n$ coordination polymers adopt a C_2-helical secondary structure along the *b*-axis with a pitch of 11.866(2) Å, and between the polymers, the tetracopper(II) cations are well trapped, with an intermolecular π–π stacking interaction between the bpy ligands and their C_2-chiral configuration regulated to be *Λ*. The present structural system could be regarded as an interesting chiral transfer mechanism mediated not by direct hydrophilic interaction between the chiral nucleotide and sugar phosphate, but by amplified hydrophobic stacking interaction between the bpy ligands.

Conclusions

The present study revealed that tetracopper(II) complexes, $[Cu_4(\mu\text{-}OH)\{\mu\text{-}(\alpha\text{-D-Glc-1P})\}_2(L)_4(H_2O)_2]^{3+}$ [L = bpy (**1**), phen (**2**)], were readily transformed into different types of nucleotide-containing coordination compounds with tetranuclear Cu^{II} aggregations, $[Cu_4(\mu\text{-}ATP)_2(bpy)_4]$ (**3**), $[Cu_4\{\mu\text{-}(IMP\text{-}H)\}_2(L)_4(H_2O)_4]^{2+}$ [L = bpy (**5**), phen (**6**)], and $\{[Cu\{\mu\text{-}(UMP\text{-}H)\}(bpy)(H_2O)]_2[Cu_4(\mu\text{-}OH)\{\mu\text{-}(\alpha\text{-D-Glc-1P})\}_2(bpy)_4(H_2O)_2]Cl\}_n$ (**7**). The structural analyses for the obtained compounds provided molecular-based important information concerning the ternary systems with Cu^{II}, nucleotide, and diimine ligand. In complex **3**, the triphosphate group of ATP exclusively assembles tetranuclear Cu^{II} ions in an unprecedented fashion and the adenine nucleobase is protected from metal binding by intramolecular stacking with a bpy moiety and intermolecular hydrogen bonding between the adenine base pairs. In addition, the crystal structure of **7** interestingly demonstrated that the C_2-helical structure of the polymer $\{[Cu\{\mu\text{-}(UMP\text{-}H)\}(bpy)(H_2O)]^-\}_n$ regulated the C_2-chiral structure of the tetranucler Cu^{II} complex cation, $[Cu_4(\mu\text{-}OH)\{\mu\text{-}(\alpha\text{-D-Glc-1P})\}_2(bpy)_4(H_2O)_2]^{3+}$, through inter- and intramolecular bpy–bpy stacking interactions.

Experimental Section

Materials: All reagents were of the best commercial grade and used as received. Complexes **1a**·$10H_2O$, **1b**·$14H_2O$, and **2**·$6H_2O$ were prepared according to the methods already reported.[13] The following abbreviations are used: adenosine 5′-triphosphate disodium salt, $Na_2[H_2ATP]$; uridine 5′-monophosphate disodium salt, $Na_2[UMP]$; inosine 5′-monophosphate disodium salt, $Na_2[IMP]$.

Measurements: Electronic absorption spectra were recorded with a Shimadzu UV-3100 spectrometer and circular dichroism spectra with a Jasco J-720 spectropolarimeter. IR spectra were measured in KBr pellets with a Jasco FTIR 410 spectrometer. The electrospray mass spectra were recorded with an Applied Biosystems model Mariner. Variable-temperature magnetic susceptibility measurements were carried out with an MPMS-5S Quantum Design SQUID magnetometer over a range of 4.5–300 K and the obtained magnetic susceptibility data were corrected for diamagnetism using Pascal's constants. Considering an idealized C_i-symmetrical structure of **3**, the four exchange parameters, J_1–J_4, were introduced to simplify the Heisenberg spin exchange Hamiltonian to $\boldsymbol{H} = -2J_1(\boldsymbol{S}_1\cdot\boldsymbol{S}_3 + \boldsymbol{S}_2\cdot\boldsymbol{S}_4) - 2J_2\boldsymbol{S}_1\cdot\boldsymbol{S}_2 - 2J_3(\boldsymbol{S}_1\cdot\boldsymbol{S}_4 + \boldsymbol{S}_2\cdot\boldsymbol{S}_3) - 2J_4\boldsymbol{S}_3\cdot\boldsymbol{S}_4$, where J_3 and J_4 were set to zero because of their long interatomic distances.

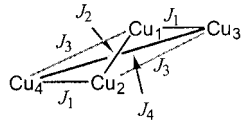

The magnetic susceptibility data were fitted by a theoretical expression derived from the van Vleck equation with the resulting energy matrix [Equation (1)], in which $A = J_1 + (1/2)J_2$, $B = -J_1 + (1/2)J_2$, $C = -(1/2)J_2 - (J_1^2 + J_2^2)^{1/2}$, $D = -(1/2)J_2 + (J_1^2 + J_2^2)^{1/2}$, and $E = (4J_1^2 + J_2^2 - 2J_1J_2)^{1/2}$. The values of *p* (ratio of paramagnetic impurity) and *Nα* (temperature-independent paramagnetism) were estimated to be 0 and 60×10^{-6} emu mol^{-1} per Cu^{II} ion, respectively.

$$\chi_M = (1-p)\left(\frac{N\mu_B^2g^2}{kT}\right)\frac{10\exp(A/kT)+2\exp(B/kT)+2\exp(C/kT)+2\exp(D/kT)}{5\exp(A/kT)+3\exp(B/kT)+3\exp(C/kT)+3\exp(D/kT)+\exp((-A-E)/kT)+\exp((-A+E)/kT)} + p\left(\frac{N\mu_B^2g^2}{kT}\right)+4N\alpha \quad (1)$$

Preparation of $[Cu_4(\mu\text{-}ATP)_2(bpy)_4]\cdot15H_2O$ (3·15H_2O): $Na_2[H_2ATP]$ (32 mg, 0.058 mmol) in CH_3OH (3 mL) was added to an aqueous solution (5 mL) of **1a**·$10H_2O$ (50 mg, 0.027 mmol). The reaction mixture was stirred at room temperature for 12 h, and was concentrated under reduced pressure to about 1 mL. Slow concentration of the solution afforded block-shaped blue crystals of $[Cu_4(\mu\text{-}ATP)_2(bpy)_4]\cdot15H_2O$ (**3**·15H_2O) in 56% yield (33 mg), which were collected and dried under vacuum. $C_{60}H_{90}Cu_4N_{18}O_{41}P_6$ (2159.50): calcd. C 33.37, H 4.20, N 11.67; found C 33.62, H 4.15, N 11.49. IR (KBr): $\tilde{\nu}$ = 3366 (br), 1653 (w), 1603 (m), 1448 (w), 1248 (s), 1100 (s), 985 (m), 906 (w) cm^{-1}. UV/Vis (H_2O): λ_{max} (ε) = 680 (1.93×10^2 M^{-1}cm^{-1}) nm. CD (H_2O): λ_{max} ($\Delta\varepsilon$) = 744 (-1.27×10^{-1}), 597 (8.15×10^{-2} M^{-1}cm^{-1}) nm.

Preparation of $[Cu_4\{\mu\text{-(IMP-H)}\}_2(L)_4(H_2O)_4](NO_3)_2\cdot nH_2O$ (5: L = bpy, n = 15; 6: L = phen, n = 20): Complex **1a**·10H_2O (61 mg, 0.030 mmol) was dissolved in H_2O (10 mL) and a portion of Na_2[IMP] (28 mg, 0.070 mmol) was added to the solution. The reaction mixture was stirred at room temperature for 12 h and was concentrated under reduced pressure to about 2 mL. Slow concentration of the solution afforded green crystals of $[Cu_4(\mu\text{-IMP})_2(bpy)_4(H_2O)_4](NO_3)_2\cdot 15H_2O$ (**5**·15H_2O), which were collected and dried under vacuum (yield 64%, 44 mg). $C_{60}H_{92}Cu_4N_{18}O_{41}P_2$ (2037.62): calcd. C 35.37, H 4.55, N 12.37; found C 35.45, H 4.04, N 11.92. IR (KBr): $\tilde{\nu}$ = 3389 (br), 1604 (s), 1385 (s), 1109 (br), 977 (m), 771 (s) cm^{-1}. UV/Vis (H_2O): λ_{max} (ε) = 671 (2.43×10^2 $M^{-1}cm^{-1}$) nm. CD (H_2O): λ_{max} ($\Delta\varepsilon$) = 693 (7.00×10^{-1} $M^{-1}cm^{-1}$) nm. MS (ESI): m/z (%) = 783.16 [calcd. for $\{Cu_4(IMP\text{-}H)_2(bpy)_4\}^{2+}$ 783.02]. A similar procedure but using complex **2**·6H_2O (59 mg, 0.032 mmol) and Na_2[IMP] (30 mg, 0.075 mmol) gave green crystals of $[Cu_4\{\mu\text{-(IMP-H)}\}_2(phen)_4(H_2O)_4](NO_3)_2\cdot 20H_2O$ (**6**·20H_2O) in 26% yield (16 mg). $C_{68}H_{102}Cu_4N_{18}O_{46}P_2$ (2223.78): calcd. C 36.73, H 4.62, N 11.34; found C 36.76, H 4.61, N 11.57. IR (KBr): $\tilde{\nu}$ = 3414 (br), 1608 (s), 1384 (s), 1106 (br), 980 (m), 772 (s) cm^{-1}. UV/Vis (H_2O): λ_{max} (ε) = 677 (3.01×10^2 $M^{-1}cm^{-1}$) nm. CD (H_2O): λ_{max} ($\Delta\varepsilon$) = 692 (4.63×10^{-1} $M^{-1}cm^{-1}$) nm. MS (ESI): m/z (%) = 831.14 [calcd. for $\{Cu_4(IMP\text{-}H)_2(phen)_4\}^{2+}$ 831.02]. The same compound with a different number of solvent water molecules, **6**·14H_2O, was prepared according to a different procedure.[8]

Preparation of $[Cu\{\mu\text{-(UMP-H)}\}(bpy)(H_2O)]_2[Cu_4(\mu\text{-OH})\{\mu\text{-}(\alpha\text{-D-Glc-1P})\}_2(bpy)_4(H_2O)_2]Cl\cdot 9H_2O$ (7·9H_2O): A portion of Na_2[UMP] (28 mg, 0.076 mmol) was added to an aqueous solution (5 mL) containing **1b**·14H_2O (106 mg, 0.059 mmol). After stirring for 12 h, the solution was concentrated under reduced pressure to about 2 mL. Slow concentration of the solution afforded blue crystals of $[Cu\{\mu\text{-(UMP-H)}\}(bpy)(H_2O)]_2[Cu_4(\mu\text{-OH})\{\mu\text{-}(\alpha\text{-D-Glc-1P})\}_2(bpy)_4(H_2O)_2]Cl\cdot 9H_2O$ (**7**·9H_2O), which were collected and dried under vacuum (yield 30% based on Cu, 32 mg). $C_{90}H_{117}ClCu_6N_{16}O_{50}P_4$ (2763.62): calcd. C 39.11, H 4.27, N 8.11; found C 39.10, H 4.20, N 8.40. IR (KBr): $\tilde{\nu}$ = 3400 (br), 1637 (s), 1447 (s), 1117 (br), 986 (m), 774 (m) cm^{-1}. UV/Vis (H_2O): λ_{max} (ε) = 658 (2.66×10^2 $M^{-1}cm^{-1}$) nm. CD (H_2O): λ_{max} ($\Delta\varepsilon$) = 708 (-1.86×10^{-2}), 601 (0.58×10^{-2}), 465 (0.24×10^{-2} $M^{-1}cm^{-1}$) nm.

Crystallographic Studies: Slow concentration of aqueous solutions afforded X-ray-quality crystals of **3**·20.5H_2O, **6**·21.5H_2O, and **7**·22H_2O, which were quickly coated with Paraton N oil and mounted on a glass fiber at low temperature. Crystal data and experimental conditions are summarized in Table 4. All data were collected at –120 °C with a Rigaku AFC8R/Mercury CCD diffractometer equipped with graphite-monochromated Mo-K_α radiation using a rotating-anode X-ray generator. A total of 2160 oscillation images, covering the whole sphere of $2\theta < 55°$, were collected with exposure rates of 120 (**3**, **6**) and 128 (**7**) s/° by the ω-scan method ($-62° < \omega < 118°$) with $\Delta\omega = 0.25°$. The crystal-to-detector (70×70 mm) distance was set to 60 mm. The data were processed using the Crystal Clear 1.3.5 program (Rigaku/MSC)[19] and corrected for Lorentz polarization and absorption effects. The structures of complexes **3**, **6**, and **7** were solved by direct methods (SIR-92/97 for **3** and **7**; DIRDIF94 Patty for **6**),[20,21] and refined on F^2 with full-matrix least-squares techniques with SHELXL-93/97.[22] In the refinement of **3**, all non-hydrogen atoms, except the solvent water oxygen atoms, were refined with anisotropic thermal parameters. The solvent water O atoms were refined isotropically. The carbon- and nitrogen-bound hydrogen atoms were placed in ideal positions, and the hydrogen atoms of the D-ribose hydroxy groups were determined from difference Fourier syntheses (H atom bound to O1 was not determined). All hydrogen atoms were fixed in the refinement. In the refinement of **6**, all non-hydrogen atoms, except the nitrate anions and the solvent water oxygen atoms, were refined with anisotropic thermal parameters. The solvent water O atoms were refined isotropically. The two nitrate anions were disordered and refined with the four-site model at special positions, each possessing 0.5 occupancy. The carbon-bound hydrogen atoms were placed at ideal positions, and the hydrogen atoms of the D-ribose hydroxy groups were determined from difference Fourier syntheses. All hydrogen atoms were fixed in the refinement. In the refinement of **7**, the Cu, Cl, and P atoms were refined anisotropically and other non-hydrogen atoms were refined with isotropic temperature factors. The positions of C–H hydrogen atoms were calculated and

Table 4. Experimental and crystallographic data for **3**·20.5H_2O, **6**·21.5H_2O, and **7**·22H_2O.

	3·20.5H_2O	**6**·21.5H_2O	**7**·22H_2O
Empirical formula	$C_{60}H_{97}Cu_4N_{18}O_{46.5}P_6$	$C_{68}H_{103}Cu_4N_{18}O_{47.5}P_2$	$C_{90}H_{143}ClCu_6N_{16}O_{63}P_4$
M_r [g mol^{-1}]	2254.55	2248.79	2997.81
Crystal system	triclinic	orthorhombic	monoclinic
Space group	$P\bar{1}$ (No.1)	$C222_1$ (No. 20)	$C2$ (No. 5)
a [Å]	10.9106(2)	19.3511(8)	33.349(1)
b [Å]	12.7652(4)	24.339(1)	11.8659(4)
c [Å]	17.4061(2)	40.127(2)	16.1861(5)
α [°]	76.852(6)	90	90
β [°]	72.075(6)	90	101.7562(4)
γ [°]	84.895(7)	90	90
V [Å^3]	2245.7(1)	18899(1)	6270.7(4)
Z	1	8	2
T [°C]	–120.0	–120	–120
μ(Mo-K_α) [cm^{-1}]	11.49	10.28	11.76
$D_{calcd.}$ [g cm^{-3}]	1.667	1.581	1.588
2θ range [°]	$6 < 2\theta < 55$	$6 < 2\theta < 55$	$6 < 2\theta < 55$
No. of observations [$I > 2\sigma(I)$]	9142	9959	5794
No. of variables	1112	1118	395
R[a]	0.037	0.051	0.074
wR_2[b]	0.100	0.148	0.196
Gof	1.01	1.00	1.05

[a] $R = \Sigma||F_o| - |F_c||/\Sigma|F_o|$. [b] $wR_2 = \{\Sigma[w(F_o^2 - F_c^2)^2]/\Sigma w(F_o^2)^2\}^{1/2}$.

were fixed in the refinement. The O–H hydrogen atoms were not determined. The Cl atom is disordered at two positions with each having 0.25 occupancy. The absolute configurations for the structures of **3**, **6**, and **7** were determined by using the chiral carbon centers of the sugar moieties, α-D-glucose and/or D-ribose units, as internal references, which was further confirmed by consistency with Flack parameters. All calculations were carried out with a Pentium PC with the Crystal Structure package 3.6[23] and a Silicon Graphics O2 station with the teXsan crystallographic software package.[24] CCDC-239857 (for **3**), -294065 (for **6**), and -294066 (for **7**) contain the supplementary crystallographic data for this paper. These data can be obtained free of charge from The Cambridge Crystallographic Data Centre via www.ccdc.cam.ac.uk/data_request/cif.

Acknowledgments

This work was partially supported by a Grant-in-Aid for Scientific Research from the Ministry of Education, Culture, Supports, Science, and Technology of Japan. A. K. S. is grateful to the Japan Society for the Promotion of Science (JSPS) for providing a fellowship and research grant.

[1] a) D. E. Wilcox, *Chem. Rev.* **1996**, *96*, 2435–2458; b) J. A. Cowan, *Chem. Rev.* **1998**, *98*, 1067–1088; c) B. L. Vallee, D. S. Auld, *Biochemistry* **1993**, *32*, 6493–6500; d) D. E. Fenton, H. Okawa, *J. Chem. Soc., Dalton Trans.* **1993**, 1349–1357; e) N. Strater, W. N. Lipscomb, T. Klabunde, B. Krebs, *Angew. Chem. Int. Ed.* **1996**, *35*, 2024–2055; f) L. S. Beese, T. A. Steitz, *EMBO J.* **1991**, *10*, 25–33; g) T. A. Steitz, S. J. Smerdon, J. Jager, C. M. Joyce, *Science* **1994**, *266*, 2022–2025; h) T. A. Steitz, J. Steitz, *Proc. Natl. Acad. Sci. U S A* **1993**, *90*, 6498–6502.

[2] a) J. E. Walker, *Angew. Chem. Int. Ed.* **1998**, *37*, 2308–2319; b) P. D. Boyer, *Angew. Chem. Int. Ed.* **1998**, *37*, 2296–2307; c) J. A. Adams, *Chem. Rev.* **2001**, *101*, 2271–2290; d) G. M. Blackburn, M. J. Gait (Eds.), *Nucleic Acids in Chemistry and Biology*, 2nd ed., Oxford University Press, New York, **1996**; e) D. Voet, J. G. Voet, *Biochemistry*, John Wiley & Sons, Inc., NewYork, **1995**.

[3] a) S. J. Lippard, J. M. Berg, *Principles of Bioinorganic Chemistry*, University Science Books, CA, **1994**; b) J. P. Whitehead, S. J. Lippard, *Metal Ions in Biological Systems* (Eds.: A. Sigel, H. Sigel), Marcel Dekker, Basel, **1996**, vol. 32, chapter 20; c) S. E. Sheman, D. Gibson, A. H.-J. Wang, S. J. Lippard, *Science* **1985**, *230*, 412–417; d) S. E. Sheman, D. Gibson, A. H.-J. Wang, S. J. Lippard, *J. Am. Chem. Soc.* **1988**, *110*, 7368–7381.

[4] a) K. Aoki, *Metal Ions in Biological Systems* (Eds.: A. Sigel, H. Sigel), Marcel Dekker, Basel, **1996**, vol. 32, chapter 4; b) H. Sigel, *Chem. Soc. Rev.* **1993**, *22*, 255–267.

[5] a) P. Orioli, R. Cini, D. Donati, S. Mangani, *Nature* **1980**, *283*, 691–693; b) P. Orioli, R. Cini, D. Donati, S. Mangani, *J. Am. Chem. Soc.* **1981**, *103*, 4446–4452.

[6] W. S. Sheldrick, *Angew. Chem. Int. Ed.* **1981**, *20*, 460–461.

[7] a) D. S. Sigman, A. Mazumder, D. M. Perrin, *Chem. Rev.* **1993**, *93*, 2295–2316; b) G. Pratviel, J. Bernadou, B. Meunier, *Angew. Chem. Int. Ed.* **1995**, *3*, 746–769; c) W. K. Pogozelski, T. D. Tullius, *Chem. Rev.* **1998**, *98*, 1089–1108; d) K. J. Humphreys, K. D. Karlin, S. E. Rokita, *J. Am. Chem. Soc.* **2002**, *124*, 6009–6019; e) K. J. Humphreys, K. D. Karlin, S. E. Rokita, *J. Am. Chem. Soc.* **2002**, *124*, 8055–8066; f) S. Dhar, D. Senapati, P. K. Das, P. Chattopadhyay, M. Nethaji, A. R. Chakravarty, *J. Am. Chem. Soc.* **2003**, *125*, 12118–12124.

[8] R. W. Gellert, B. E. Fischer, R. Bau, *J. Am. Chem. Soc.* **1980**, *102*, 7812–7815.

[9] S. Korn, W. S. Sheldrick, *J. Chem. Soc., Dalton Trans.* **1997**, 2191–2200.

[10] L. Y. Kuo, M. G. Kanatzidis, M. Sabat, A. L. Tipton, T. J. Marks, *J. Am. Chem. Soc.* **1991**, *113*, 9027–9045.

[11] M. Inoue, T. Yamase, *Bull. Chem. Soc. Jpn.* **1996**, *69*, 2863–2868.

[12] a) K. Aoki, *J. Am. Chem. Soc.* **1978**, *100*, 7106–7108; b) K. Aoki, *J. Chem. Soc., Chem. Commun.* **1979**, 589–591; c) K. Aoki, H. Yamazaki, *J. Chem. Soc. Jpn.* **1988**, 611–620; d) R. Cini, G. Giorgi, *Inorg. Chim. Acta* **1987**, *137*, 87–90; e) G. Giorgi, R. Cini, *Inorg. Chim. Acta* **1988**, *151*, 153–161; f) B. E. Fischer, R. Bau, *Inorg. Chem.* **1978**, *17*, 27–34; g) C.-Y. Wei, B. E. Fischer, R. Bau, *J. Chem. Soc., Chem. Commun.* **1978**, 1053–1055.

[13] a) M. Kato, T. Tanase, *Inorg. Chem.* **2005**, *44*, 8–10; b) M. Kato, A. K. Sah, T. Tanase, M. Mikuriya, submitted for publication.

[14] P. E. Kruger, R. P. Doyle, M. Julve, F. Lloret, M. Nieuwenhuyzen, *Inorg. Chem.* **2001**, *40*, 1726–1727.

[15] a) R. Cini, L. G. Marzilli, *Inorg. Chem.* **1988**, *27*, 1855–1856; b) M. Sabat, R. Cini, T. Haromy, M. Sundaralingam, *Biochemistry* **1985**, *24*, 7827–7833; c) R. Cini, M. C. Burla, A. Nunzi, G. P. Polidori, P. F. Zanazzi, *J. Chem. Soc., Dalton Trans.* **1984**, 2467–2476; d) R. Cini, M. Sabat, M. Sundaralingam, M. C. Burla, A. Nunzi, G. Polidori, P. F. Zanazzi, *J. Biomol. Struct. Dyn.* **1983**, *1*, 633–637.

[16] For example: a) R. Cini, C. Pifferi, *J. Chem. Soc., Dalton Trans.* **1999**, 699–710; b) Y. Sugawara, N. Kamiya, H. Iwasaki, T. Ito, Y. Satow, *J. Am. Chem. Soc.* **1991**, *113*, 5440–5445, and references therein.

[17] W. S. Sheldrick, *Z. Naturforsch* **1982**, *37b*, 863–871.

[18] A. W. Addison, T. N. Rao, *J. Chem. Soc., Dalton Trans.* **1984**, 1349–1356.

[19] *Crystal Clear 1.3.5, Operating Software for the CCD Detector System*, Rigaku, Molecular Structure Corp., Tokyo, **2003**.

[20] a) A. Altomare, M. Burla, M. Camalli, G. Cascarano, C. Giacovazzo, A. Guagliardi, A. Moliterni, G. Polidori, R. Spagna, *J. Appl. Crystallogr.* **1999**, *32*, 115–119; b) A. Altomare, G. Cascarano, C. Giacovazzo, A. Guagliardi, M. Burla, G. Polidori, M. Camalli, *J. Appl. Crystallogr.* **1994**, *27*, 435–436.

[21] P. T. Beurskens, G. Admiraal, G. Beurskens, W. P. Bosman, R. de Gelder, R. Israel, J. M. M. Smits, *DIRDIF-94 program system*, Technical Report of the Crystallography Laboratory, University of Nijmegen, The Netherlands, **1994**.

[22] a) G. M. Sheldrick, *SHELXL-93, Program for Crystal Structure Refinement*, University of Göttingen, Göttingen, Germany, **1993**; b) G. M. Sheldrick, *SHELXL-97, Program for the Refinement of Crystal Structures*, University of Göttingen, Göttingen, Germany, **1997**.

[23] *Crystal Structure 3.6, Crystal Structure Analysis Package*, Rigaku and Molecular Structure Corp., Tokyo, **2003**.

[24] *teXsan: Crystal Structure Analysis Package*, Molecular Structure Corp., Tokyo, **1999**.

Received: January 6, 2006
Published Online: April 11, 2006

